ULTRASONIC VIBRATION MEASUREMENT USING HETERODYNE INTERFEROMETRY AND SDR PHASE METER

ĐO ĐỘ RUNG SIÊU ÂM SỬ DỤNG GIAO THOA KẾ HAI TẦN SỐ VÀ MÁY ĐO PHA SDR

Pham Van Dam[1], Nguyen The Tai[1], Nguyen Thanh Dong[1*], Vu Thanh Tung[1], Hoang Hong Hai[1], Vu Toan Thang[1] and Nguyen Thi Phuong Mai[1]

[1] School of Mechanical Engineering, Hanoi University of Science and Technology, Vietnam.

Corresponding author: Nguyen Thanh Dong (email: dong.nguyenthanh@hust.edu.vn)

Received: 11-Sep-2023; Accepted: 24-Sep-2023; Published online: 29-Sep-2023

ABSTRACT

Ultrasonic vibration measurement and the development of ultrasonic vibration sensors have a significant impact on underwater pattern detection, providing good support for the exploitation and usage of marine resources. Advanced digital signal processing algorithms improve mechanical displacement measurements using ultrasonic speed and pm-level interferometers in real-time. In recent years, developing digital algorithms and employing low-cost software-defined radio (SDR) software applied to communication systems and other general-purpose systems with flexible solutions are essential in modern industrial applications. Specifically, the SDR can be consistent with real-time phase-change measurements of MHz-frequency interference signals for a heterodyne interferometer. This paper combines a heterodyne interferometer and a real-time SDR phase meter, demonstrating an ultrasonic vibration instrument's high-speed vibrating measurement capabilities. A double-pass interferometer is implemented to produce interference signals modulated with a sine waveform phase change associated with a tool's ultrasonic vibrating displacement, calculated by the phase meter's quadrature demodulation algorithm. The measurement results show that the system detects the sine-wave vibration trajectory generated by the vibrator at a frequency of 20 kHz and an amplitude of ~460 nm. The principle of the measurement system, instrumentations, experiments, and results are discussed in the paper.

Keywords: *High-speed vibration measurement, ultrasonic sensor, heterodyne interferometry, quadrature demodulation, software-defined radio*

TÓM TẮT

Đo rung siêu âm và phát triển cảm biến rung siêu âm có tác động đáng kể đến phát hiện mô hình dưới bước, hỗ trợ tốt cho việc khai thác và sử dụng các tài nguyên biển. Các thuật toán xử lý tín hiệu số tiên tiến cải thiện các phép đo dịch chuyển cơ học bằng cách sử dụng giao thoa kế đo dịch chuyển nhỏ ở mức pi cô mét và ở tốc độ siêu âm trong thời gian thực. Trong những năm gần đây, việc phát triển các thuật toán kỹ thuật số và sử dụng phần mềm vô tuyến được định nghĩa bằng phần mềm (SDR) có chi phí thấp áp đang dụng cho các hệ thống truyền thông và các hệ thống có mục đích chung khác với các giải pháp linh hoạt là rất cần thiết trong các ứng dụng công nghiệp hiện đại. Cụ thể, SDR có thể phù hợp với các phép đo thay đổi pha theo thời gian thực với các tín hiệu giao thoa có tần số chập MHz trong giao thoa kế hai tần số (heterodyne). Bài báo trình bày sự kết hợp giao thoa kế hai tần số và máy đo pha SDR trong thời gian thực có khả năng đo rung tốc độ cao của thiết bị rung siêu âm. Một giao thoa kế đường truyền kép (double-pas interferometer) được triển khai để tạo ra các tín hiệu giao thoa được mô đun pha dạng sóng sin liên quan đến sự dịch chuyển rung siêu âm dạng sóng sin của dao công cụ và sự mô đun pha được tính bằng thuật toán điều chế hai pha cùng tần số nhưng lệch pha nhau 90 độ (quadrature modulation) của máy đo pha. Kết quả đo cho thấy hệ thống đo phát hiện quỹ đạo dao động sóng hình sin do máy rung của dụng cụ cắt tạo ra ở tần số 20 kHz và biên độ ~460 nm. Nguyên lý của hệ thống đo lường, thiết bị đo, thí nghiệm và kết quả được thảo luận trong bài báo.

Từ khóa: *Đo rung tốc độ cao, cảm biến siêu âm, giao thoa kế hai tần số, điều chế pha cùng tần số nhưng lệch pha 90 độ, sóng vô tuyến định nghĩa bằng phần mềm*

I. INTRODUCTION

For decades, ultrasonic vibrating applications have been considered a powerful support for cutting hard materials and increasing machining accuracy and cutting tool duration in cutting, milling, or drilling processes [1,2]. Otherwise, ultrasonic vibration and ultrasonic sensors have attracted much attention from researchers since the first sea trials were performed using fiber optic hydrophones [3]. The research of ultrasonic sensors has a significant impact on underwater pattern detection, greatly helping its reasonable exploitation and comprehensive usage of marine resources [4–6].

Interferometry has been utilized in many fields since Michelson invented the first configuration. Nowadays, the interferometer plays a crucial role in the semiconductor industry, precision mechanics, or other science fields. The main reason is that it provides a noncontact method with a pm-measurement level by extracting information from interference. By using light as a reference tool, interferometry can reach a high-velocity response, but it becomes a burden for signal processing part or device capability, such as expensive megahertz sampling rate analog-to-digital converter (ADC). There are many configurations of interferometer systems, such as homodyne interferometers, heterodyne interferometers [7], multi-beam interferometers [8], frequency-modulated interferometers [9], and so forth. All these types are developed for several features of usages such as high-resolution, high-speed, 3D surface measurements. In the world, a commercial laser Doppler vibrometer of the Polytech brand is famous for vibration measurement, but it has drawbacks, such as being unable to display vibration forms or low-frequency measurement for high accuracy [10]. However, our primary efforts have been devoted to mechanical measurement manufacture, and ultrasonic vibration measurement is one of them, where a heterodyne interferometer is a potential candidate for extracting high resolution with low-noise signals and high stability.

Since a radio signal receiver (SDR - software-defined radio) was discovered for high-frequency signal processing of heterodyne interferometer [11,12], it opens a new technology for real-time heterodyne interferometer signal processing. The RTL-SDR is a low-cost software-defined radio that can be used efficiently as a receiver and transmitter with a wide range of frequencies, especially for radio communication. Besides, due to its open-source nature, developers have been able to create software that runs on various platforms, allowing users to benefit from the full capabilities of the RTL-SDR. GNU Radio is controlled by a personal computer (PC), which can process signals in real-time, while it is a free and open-source software development toolkit that provides signal processing blocks to implement software radios written in either C++ or Python programming language. It can be used with readily - available low-cost external radio frequency hardware (RTL-SDR dongle) to create software-defined radios [13]. SDR implementations have been used in different applications, such as cognitive radio [14], low-power and cost transceivers [15], coherent radar systems [16], and dual-comb spectrometers [17].

In this paper, we develop a phasemeter using an RTL-SDR dongle and GNU Radio software for a double-pass heterodyne system to evaluate the working operation of a vibrator (20 kHz frequency vibration). The experiment demonstrates that the combination with the SDR phasemeter and the heterodyne interferometer system can do a real-time vibration measurement with an amplitude of ~460 nm at 20 kHz. The results of the phasemeter will be compared with those of a laboratory phasemeter with a high sampling rate (20 MHz) and calculated point-by-point.

Overall, we present an orientation of heterodyne interferometer theory, the SDR phasemeter principle, and our practical experiment in Section 2. In Section 3, we discuss the results, advantages, and disadvantages of our system.

II. METHODOLOGY

1 Heterodyne interferometer principle

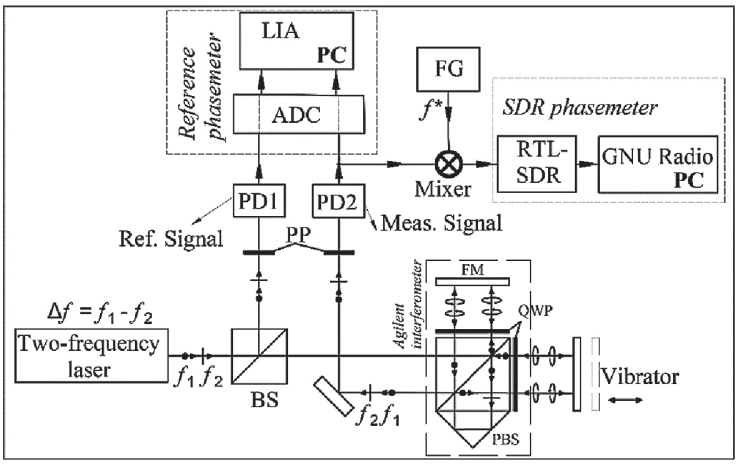

Fig. 1. Simulation of basic optical heterodyne interferometer systems using double-pass interferometer.

BS, beam splitter; PBS, polarization beam splitter; QWP, quarter-wave plate; PD1&2, photodetectors; PC, personal computer; ADC, analog-to-digital converter; FG, function generator; LIA, lock-in amplifier [9].

Our proposed setup contains a frequency-stabilized He-Ne laser (Fig. 1), which has two slightly different and orthogonally polarizing frequencies, f_1 and f_2, a beam splitter (BS), double-pass interferometer, two polarization plates (PP) and two photodetectors (PDs). When the laser beam travels through the BS, the laser beam is separated into reflected and transmitted beams. Firstly, reference signal Ir is generated by the reflected beam passing through PP towards PD1. Secondly, the transmitted beam enters a double-pass interferometer. The laser beam is reflected twice before it goes into the PD2. By adjusting the PP polarization axis to an angle of 45º to the polarization plane of the beams f_1 and f_2, the interference signal Im is generated at PD2 reached the maximum. Finally, phase meters are built to process these signals for extracting the displacement of the motioning object.

As the optical path differences (OPD) change to fractions of wavelengths, the corresponding interference phase changes proportionally. These phase changes are directly proportional to the change in OPD. Based on the optical configuration below, the relation between the displacement L and different phase θ_m (in radian) can be determined by the below formula [18,19]:

$$\theta_m = \frac{8\pi n}{\lambda} L \qquad (1)$$

where n is the environmental index, λ is the wavelength of the laser source.

In the heterodyne interferometer, $\omega_m = 2\pi f_m$ is the angular frequency of the interferometer pattern, and θ_m is the different phase of two signals, including a measurement signal I_m (B amplitude) and a reference signal I_r (A amplitude) described as [18]:

$$I_r = A\sin(\omega_m t), \qquad (2)$$

$$I_m = B\sin(\omega_m t + \theta_m) \qquad (3)$$

In the next part, based on Eq. (2) and (3), our phasemeters will find the phase change to determine the corresponding displacement.

2. SDR phasemeter using RTL-SDR dongle and GNU Radio

Our testing phasemeter combines both analog and digital signal processing that are responded to by the R820T tuner working as an analog downbeat system and RTL2832U, providing an ADC 28.8 MHz sampling clock, respectively [12,20,21]. At the next stage, the low-frequency signal is processed to determine its phase by the quadrature demodulation

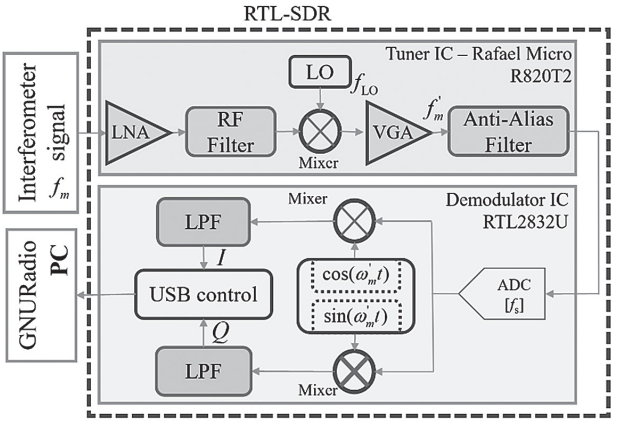

Fig. 2. Schematic of signal processing.

SDR, software-defined radio; LO, local oscillator; LNA, low noise amplifier; VGA, variable gain amplifier; ADC, analog-to-digital converter; LPF, low-pass filter; USB control, universal serial bus control; PC, personal computer.

method, which works on GNU Radio software.

The incident optical power of the heterodyne interferometer system is converted to a voltage by a photodiode proportionally, and RTL-SDR receives them. In analog signal processing, the amplitude signal $I_m(t)$ is increased by a low-noise gain, mixed with a local oscillator (LO) signal to generate the output $I'_m(t)$. Here f_{LO} in $I_m(t)$ can be chosen automatically from 25 MHz to 1766 MHz to tune down a lower frequency f'_m ($f'_m = f_m - f_{LO}$) in $I'_m(t)$ [20].

The down-beat frequency technique can be described below:

$$I_m(t) \times \cos(\omega_{LO} t) = \frac{1}{2} B \sin(\omega_m t + \omega_{LO} t + \theta_m) + \frac{1}{2} B \sin(\omega_m t - \omega_{LO} + \theta_m) \quad (4)$$

Passing through a low-pass filter (LPF) to remove a high-frequency term, $I'_m(t)$ is

$$I'_m(t) = \frac{1}{2} B \sin(\omega_m t - \omega_{LO} + \theta_m) = \frac{1}{2} B \sin(\omega'_m + \theta_m) \quad (5)$$

In the digital processing stage, the signals are converted to digital signals by the ADC of RTL2832U with a sampling rate f_s = 28.8 MHz [13], and the main RTL2832U task is described in **Fig. 2** [12].

$$I'_m(t) \cdot \sin(\omega'_m t) = -\frac{1}{4} B \cos(2\omega'_m t + \theta_m) + \frac{1}{4} B \cos(\theta_m) \quad (6)$$

$$I'_m(t) \cdot \cos(\omega'_m t) = \frac{1}{4} B \sin(2\omega'_m t + \theta_m) + \frac{1}{4} B \sin(\theta_m) \quad (7)$$

By using LPFs to cut off high-frequency signals, Eq. (6) and (7) can be re-written as:

$$I(t) = \frac{1}{4} B \sin(\theta_m) \quad (8)$$

$$Q(t) = \frac{1}{4} B \cos(\theta_m) \quad (9)$$

In the next stage, the PC program in the GNU radio software acquires the signals $I(t)$ and $Q(t)$ from the RTL-SDR device to the PC via USB access at a stable sample rate of 2.4 MS/s [21]. In this program, due to performing in the multi-frequency environment and preventing the program from overloading, the rational sampler function reduces the sampling frequency of $I(t)$ and $Q(t)$ by five times and is equal to 480 kHz. Then, the quadrature demodulation function calculates the argument (angle, in radians) of $I(t)$ and $Q(t)$ to generate the phase θ_m [20,22,23]. θ_m is filtered by a bandpass filter ranging from 18 to 22 kHz to remove redundant frequency components. Finally, the output is converted to introduce the displacement L.

III. EXPERIMENTS AND RESULTS

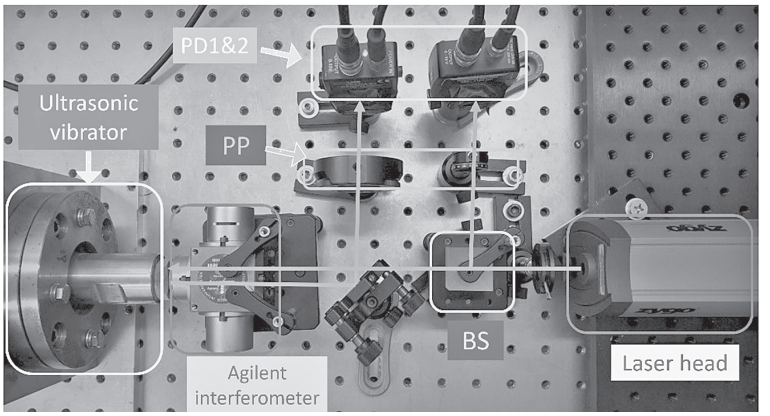

Fig. 3. Practical experiment of ultrasonic measurement.

BS, beam splitter; PP, polarization plate; PD, photodetector.

In our practical experiment, the laser beam is generated by a frequency-stabilized He-Ne laser (Zygo ZMI-7705 3.6 MHz frequency and 633 nm wavelength [24]), which is collected by PDA36A photodiodes (Thorlabs, 12 MHz bandwidth [25]) and a double-pass interferometer Agilent 10706B [26] to increase the resolution of phase detection. The measurement signal is mixed with a pure signal from a function generator, which will then be proceeded by the SDR phasemeter. In Fig. 3, an ultrasonic vibrator is controlled by a high-voltage driver and screwed into an anti-vibration optical table workstation. The main engine of the vibrator is a PZT actuator driven by a high-frequency voltage at 20 kHz; hence, the vibrating can be generated only in one axis. The whole optical system is set close to reduce dead-path and environmental effects.

Two phase meters will process the interferometer signals (a reference one is built by our laboratory and the SDR one). The reference phase meter is based on a lock-in amplifier method at a 20 MHz sampling rate, which works concurrently with the SDR phase meter. Both the results agree that the measured vibration amplitudes are ~460 nm at 19930 Hz with ~0.262 nm standard deviation within 0.5 µs (Fig. 4).

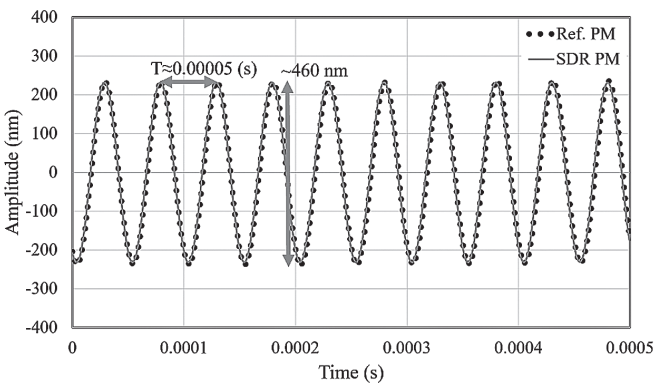

Fig. 4. Measurement results of reference and SDR phase meters.

IV. CONCLUSION

This paper presents ultrasonic vibration measurement using a heterodyne interferometer with our phasemeter and phasemeter based on SDR. As a result, the SDR phase meter has been constructed by GNU Radio software, which can process interferometer signals in real time and shows the same results as our reference

phase meter (0.262 nm standard deviation). Our practical experiment is implemented on the ultrasonic vibrator with a vibration amplitude of ~460 nm at ~20 kHz.

The main limitation of the RTL-SDR is the scarcity of references that provide a complete description of its operation. Although the functionality of the RTL-SDR is limited (primarily developed for digital video and radio applications using the mid-band), ultrasonic vibration/displacement measurements can be measured for heterodyne interferometry. Even though we have not determined the error of measurement results, we partly avoid the environmental effects. One of the most significant advantages is that the SDR phase meter can be built with an affordable RTL-SDR dongle and a PC for real-time measurements. Hence, due to these points, our phase meter can be applied in industrial manufacturing. Besides, the RTL SDR uses low-resolution ADC, so it is difficult to perform high-speed phase measurements with resolution and stability below tens of millidegrees, and thus, pm-order displacement measurements may be limited from signal processing. In the future, we are trying to upgrade the optical system to reduce noise and integrate a vibration measurement system on machines. Therefore, our research can contribute to checking and evaluating product quality.

ACKNOWLEDGMENTS

This research is funded by Hanoi University of Science and Technology (HUST) under project number T2022-TT-003.

REFERENCES

1. Kumar, S., Wu, C. S., Padhy, G. K., Ding, W., Application of ultrasonic vibrations in welding and metal processing: A status review. Journal of Manufacturing Processes 26 (2017) 295-322.
2. Yang, Z., Zhu, L., Zhang, G., Ni, C., Lin, B., Review of ultrasonic vibration-assisted machining in advanced materials. International Journal of Machine Tools and Manufacture (2020).
3. T. Yoshino, K. Kurosawa, K. Itoh, T. Ose, Fiber-optic Fabry-Perot interferometer and its sensor applications, IEEE J. Quantum Electron. 18 (10) (1982) 1624–1633.
4. J. Li, Z.L. Liu, F.D. Liu, Using sub-resolution features for self-compensation of the modulation transfer function in remote sensing, Opt. Exp. 25 (4) (2017) 4018–4037.
5. F. Eric, M.D. Santos, C.K. Suzuki, Optical fiber specklegram sensor analysis by speckle pattern division, Appl. Opt. 56 (2017) 1585–1590.
6. L.M. Riobo, F.E. Veiras, P.A. Sorichetti, M.T. Garea, Wideband quad optical sensor for high-speed subnanometer interferometry, Appl. Opt. 56 (2017) 397–403.
7. (Spie Field Guides) Jonathan D. Ellis - Field Guide to Displacement Measuring Interferometry-Society of Photo-Optical (2014)
8. Hall, A. C., Multiple-beam interferometry, Characterization of Solid Surfaces (1974) 33–48. doi:10.1007/978-1-4613-4490-2_3
9. Vu, T.-T., Higuchi, M., & Aketagawa, M., Accurate displacement-measuring interferometer with wide range using an I_2 frequency-stabilized laser diode based on sinusoidal frequency modulation. Measurement Science and Technology 27(10) (2016) 105201.
10. https://www.polytec.com/int/vibrometry/products/special-application-vibrometers/hsv-100-high-speed-vibrometer.
11. RTL-SDR Blog V3, RTL-SDR blog V3 datasheet, http://www.rtl-sdr.com/wp-content/uploads/2017/06/

RTL-SDR-Blog-V3-Datasheet.pdf

12. L. M. Riobo, F. E. Veiras, M. G. Gonzalez, M. T. Garea, P. A. Sorichetti, High-speed real-time heterodyne interferometry using software-defined radio 57(2) (2018) 217-224.
13. G. Proyect, Gnu radio, https://www.gnuradio.org.
14. H. Sun, A. Nallanathan, C.-X. Wang, and Y. Chen, Wideband spectrum sensing for cognitive radio networks: a survey, IEEE Wireless Commun. 20 (2013) 74–81.
15. J. W. Jeong, A. Nassery, J. N. Kitchen, S. Ozev, Built-in self-test and digital calibration of zero-IF RF transceivers," IEEE Transactions on Very Large Scale Integration (VLSI) Systems, 24(6) (2016) 2286-2298. doi: 10.1109/TVLSI.2015.2506547.
16. J. R. Mediavilla, C. A. Espinoza, A. P. Espinosa, F. Salazar, Design of a passive radar based on RTL-SDR technology with coherent dual channel, J. Phys.: Conf. Ser. 2199 (2022) 012023.
17. C. Quevedo-Galán, A. Pérez-Serrano, I. E. López-Delgado, J. M. G. Tijero, I. Esquivias, Dual-comb spectrometer based on gain-switched semiconductor lasers and a low-cost software-defined radio, in IEEE Access 9 (2021) 92367-92373.
18. T.-D Nguyen, Q.-A. Duong, M. Higuchi, T.-T. Vu, D. Wei, M. Aketagawa, 19-picometer mechanical step displacement measurement using heterodyne interferometer with phase-locked loop and piezoelectric driving flexure-stage, Sens. Actuators A Phys. 304 (2020), 111880.
19. Richard Leach, Fundamental principles of engineering nanometrology, Second Edition, 2014.
20. Realtek, Rtl2832u: DVB-T COFDM Demodulator+USB 2.0, http://www.realtek.com.tw/products/productsView.aspx?Langid=1&PFid=35&Level=4&Conn=3&ProdID=257. RTL-SDR Blog V3 Datasheet.pdf https://www.rtl-sdr.com/wp-content/uploads/2018/02/RTL-SDR-Blog-V3-Datasheet.pdf
21. Rafael Micro, Rafael micro R820T2 tuner datasheet, http://www.rtl-sdr.com/wp-content/uploads/2013/04/R820T_datasheet-Non_R-20111130_unlocked1.pdf.
22. Faulkner, E., Yun, Z., Zhou, S., Shi, Z. J., Han, S., Giannakis, G. B., An Advanced GNU Radio Receiver of IEEE 802.15.4 OQPSK Physical Layer. IEEE Internet of Things Journal, 8(11) (2021) 9206–9218.
23. Feng Ge, Chiang, C. J., Gottlieb, Y. M., Chadha, R., GNU Radio-Based Digital Communications: Computational Analysis of a GMSK Transceiver. IEEE Global Telecommunications Conference - GLOBECOM (2011).
24. ZYGO, ZMI 7705 Laser head specifications, https://www.lambdaphoto.co.uk/pdfs/Zygo/LAMBDA_zmi-7705-laser-head-specs.pdf.
25. Thorlabs, PDA36A Si-Amplified Detectors, https://www.thorlabs.com/thorProduct.cfm?partNumber=PDA36A.
26. Keysight, 10706B High Stability Plane Mirror Interferometer https://www.keysight.com/us/en/product/10706B/high-stability-plane-mirror-interferometer.html